Article

A Dual Optimization Approach to Bimetallic Nanoparticle Catalysis: Impact of M1:M2 Ratio and Supporting Polymer Structure on Reactivity

Venkatareddy Udumula, Jefferson H. Tyler, Donald L. Davis, Hao Wang, Matthew R. Linford, Paul S. Minson, and David J. Michaelis

ACS Catal., **Just Accepted Manuscript** • DOI: 10.1021/acscatal.5b00830 • Publication Date (Web): 27 Apr 2015

A Dual Optimization Approach to Bimetallic Nanoparticle Catalysis: Impact of M_1:M_2 Ratio and Supporting Polymer Structure on Reactivity

Venkatareddy Udumula, Jefferson H. Tyler, Donald L. Davis, Hao Wang, Matthew R. Linford, Paul S. Minson, David J. Michaelis*

Department of Chemistry and Biochemistry, Brigham Young University, Provo, UT 84602

ABSTRACT: A dual optimization approach to nanoparticle catalysis is reported where both the composition of a bimetallic nanoparticle and the electronic properties of the supporting polystyrene-based polymer can be varied to optimize reactivity and chemoselectivity in nitroarene reductions. Ruthenium-cobalt nanoparticles supported on polystyrene are shown to catalyze nitroarene reductions at room temperature with exceptional activity as compared to monometallic ruthenium catalysts. Both the identity of the second metal and the M_1:M_2 ratio show a profound effect on the chemoselectivity of nitroarene reductions. These polymer-supported bimetallic catalysts are shown to react with nearly complete chemoselectivity for nitro group reduction over a variety of easily reducible functional groups. The electronic properties of the supporting polymer also have a significant impact on catalysis, where electron-deficient polystyrenes enable 100% conversion to the aniline product in just 20 minutes at room temperature. Polymer effects are also shown to influence the mechanism of the reduction reaction, in addition to accelerating the rate, confirming the impact of the polymer structure on catalytic efficiency. These catalysts are easily prepared in a single step from commercial materials and can be readily recycled without loss of activity.

Key Words: Bimetallic Nanoparticle, nitroarene reduction, catalysis, polymer support, metal-support interaction

Introduction

Nanoparticle catalysis has emerged in the last decade as an effective method for generating high surface area, efficient, and recyclable heterogeneous catalysts for organic synthesis.[1] Much of this work has involved formation of nanoparticle catalysts supported on metal oxide supports and porous zeolite materials that aid in controlling the size and agglomeration state of the nanoparticle catalysts.[2] The nature of the support can often affect the catalytic activity of the deposited metal catalyst in positive ways through formation of what are known as strong metal–support interactions.[3] While modification of the solid support can be used to optimize catalytic activity, such modifications can be challenging to make.[4] It is often even more difficult to predict how changes to the solid support will impact the catalytic activity of the supported metal catalysts.

The Kobayashi laboratory has pioneered methods for generating polymer-stabilized nanoparticle catalysts (Figure 1).[5] In these catalysts, reactivity can be optimized by incorporation of supporting ligands into the polymer structure,[5d, 6] or by formation of mixed metal nanoparticles.[7,8] The development of mixed metal nanoparticle catalysts is a well known approach to improve catalyst performance because a second metal can change the crystal structure and/or change the electronic properties of the metal catalyst.[9] Our laboratory is interested in the potential of novel metal-polymer interactions to tune the catalytic activity of nanoparticle catalysts in predictable ways. This approach has the potential to streamline catalyst optimization in heterogeneous catalysis, similar to what is accomplished through ligand modification in homogeneous transition metal catalysis.[10] Herein we report the development of polystyrene-supported Ru-Co bimetallic nanoparticle catalysts via a dual optimization approach where both the nanoparticle composition (M_1:M_2 ratio) and polymer electronic structure contribute to exceptional catalyst activity in nitroarene reductions that proceed at room temperature (Figure 1). We demonstrate that variation of the electronic character of the aryl rings on the polymer support via incorporation of electron-donating and electron-withdrawing substituents can lead to predictable changes in catalytic activity. The polymer structure is shown to not only affect the rate of catalysis, but also to influence the mechanism of the transformation. To the best of our knowledge, this is the first example where the electronic properties of a supporting polymer have been shown to influence the activity of incorporated nanoparticle catalysts in predictable ways.[10–12]

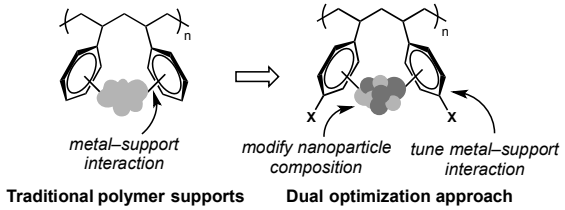

Figure 1. Polymer-supported nanoparticle catalysts

The reduction of nitroarenes is a widely used process for generating anilines, which are often found in specialty chemicals and pharmaceuticals.[13] Nanoparticle-catalyzed nitroarene reductions are particularly important because the catalysts exhibit exceptional reactivity, are easily recovered after the reaction, and can often be recycled.[14] We chose nitroarene reductions as a model reaction for our optimization studies due

to the importance of the transformation industrially and the challenge of performing chemoselective reductions in the presence of other easily reduced functional groups.[13d] Our objective in exploring the reactivity of polymer-supported nanoparticle catalysts in nitroarene reductions was to develop an inexpensive, easily synthesized and recyclable catalyst that enables reductions at room temperature.[15]

Results and Discussion

We began our optimization studies with ruthenium nanoparticles due to their known potential to perform nitroarene reductions.[16] The nanoparticle catalysts were synthesized according to a reported procedure via reduction of the respective metal salt(s) with sodium borohydride in the presence of a homogeneous solution of polystyrene (MW 25000, Figure 2).[5a] The nanoparticle-polymer composites were then precipitated from solution, washed to remove unsupported particles and salts, dried under vacuum, and used without further processing. The resulting dark powders are easy to manipulate and can be readily recovered from the reaction mixtures by simple filtration. In addition, all materials used in the synthesis of these catalysts are available from commercial sources.

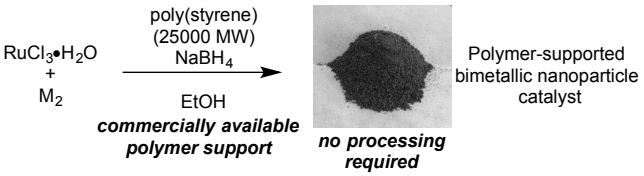

Figure 2. Synthesis of bimetallic nanoparticle catalysts.

Nanoparticle catalysts thus prepared were found to have high activity for nitroarene reductions at room temperature in ethanol with hydrazine hydrate as the stoichiometric reductant (Table 1). Ethanol was an ideal solvent for these reductions as the nanoparticle catalysts remained heterogeneous and could be easily removed after the reaction by filtration. When the monometallic ruthenium nanoparticle catalyst was used for reduction of 3-nitrostyrene, a mixture of product and partially reduced byproducts was obtained (entry 1). While good chemoselectivity for reduction of the nitro functional group was observed, the low activity of the catalyst resulted in formation of a variety of partially reduced byproducts upon complete consumption of the reductant. We then explored the potential of bimetallic Ru–M nanoparticles to increase reactivity and chemoselectivity.[7,9] While copper (entry 2) and nickel (entry 3) did not lead to improved catalysis, iron and cobalt bimetallic catalyst (entry 4–5) provided exceptional activity and selectivity under these mild reduction conditions.[7f] Our continuing studies focused on Ru-Co nanoparticle catalysts because they were found to be more chemoselective than the corresponding Ru-Fe nanoparticles (see supporting information. We next investigated the impact of the ratio of the two metals on catalysis (Table 1, entries 6–9). These studies showed that a higher percentage of ruthenium to cobalt led to a more active catalyst when the total loading of ruthenium was held constant in the reaction at 2 mol% (entry 9). This polystyrene-supported Ru–Co bimetallic catalysts ($5.1\%(_{81}Ru_{19}Co)/PS$)[9d] is among the most active nanoparticle catalysts for nitroarene reductions, proceeding in just under two hours at room temperature.[14]

Table 1. Catalyst Optimization Studies

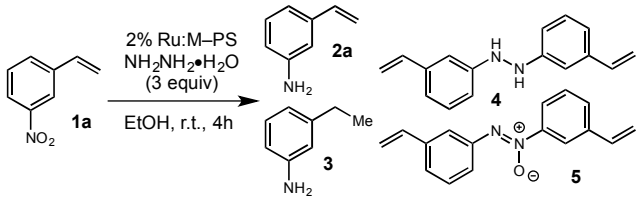

entry[a]	catalyst	catalyst composition[b,c]	% conv.[d]	selectivity (2:3:4:5)[c]
1	Ru	$6.7\%(_{100}Ru)/PS$	100	60:0:18:22
2	Ru : Cu	$5.4\%(_{51}Ru_{49}Cu)/PS$	100	63:4:32:1
3	Ru : Ni	$6.7\%(_{44}Ru_{56}Ni)/PS$	100	41:2:32:25
4	Ru : Fe	$7.0\%(_{24}Ru_{76}Fe)/PS$	100	95:4:0:1
5	Ru : Co	$5.6\%(_{46}Ru_{54}Co)/PS$	100	83:14:0:3
6	Ru : Co	$3.6\%(_{61}Ru_{39}Co)/PS$	100	28:10:14:48
7	Ru : Co	$5.7\%(_{35}Ru_{65}Co)/PS$	100	45:8:0:47
8	Ru : Co	$7.8\%(_{23}Ru_{77}Co)/PS$	100	17:8:25:50
9	Ru : Co	$5.1\%(_{81}Ru_{19}Co)/PS$	100	97:3:0:0

[a] Reactions conditions: **1a** (0.4 mmol), catalyst (2 mol% wrt Ru), and $NH_2NH_2•H_2O$ (3 equiv) in EtOH at room temp. [b] Catalyst composition represented as n%(xM1yM2)/support, where n is total wt% metals in support, and x and y are the relative wt% of M1 and M2. [c] Metal ratios determined by ICP analysis (see supporting information). [d] Determined by ^1H NMR analysis of the crude reaction mixture. PS = polystyrene, MW 25,000.

With highly active nanoparticle catalysts in hand, we next investigated their functional group tolerance and chemoselectivity in a variety of nitroarene reductions. In all cases, the aniline products were obtained in near quantitative yield after simply filtering off the catalyst and evaporating the solvent (Table 2). Aromatic olefins (entries 1–3), halides (entries 4–8), cyanides (entry 9), carboxylic acids (entry 10), phenols (entry 11), and carbonyl functionalities (12–15) were all tolerated in the reaction. Dinitro aromatics also readily reduced to provide the diamine products (entries 16–17). Other easily reducible functional groups were also tolerated, including alkynes (entries 18, 19), allyl ethers (entry 20), stilbenes (entry 21), and Lewis basic heterocycles (entries 22, 23).

We next desired to determine whether our nanoparticle catalysts could be recovered and recycled for subsequent reactions (Scheme 1). The poly(styrene)-supported Ru:Co nanoparticles remain heterogeneous when the reduction reaction is conducted in ethanol and can be easily recovered by simple filtration after complete consumption of the starting material.

Table 2. Substrate scope of nitroarene reduction.

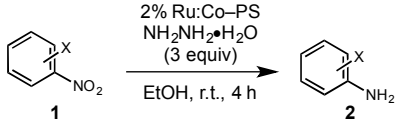

entry[a]	Substrate (**1**)		2	Yield/ Select.[b]
1	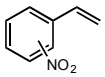	3-NO_2 **1a**	**2a**	96/97
2		4-NO_2 **1b**	**2b**	97/97
3		2-NO_2 **1c**	**2c**	97/97
4		4-Cl **1d**	**2d**	98/99
5		2-Cl **1e**	**2e**	99/99
6		**4-F 1f**	**2f**	96/99
7		4-Br **1g**	**2g**	97/99
8		**4-I 1h**	**2h**	98/99
9		4-CN **1i**	**2i**	98/99
10[c]	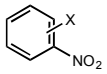	4-COOH **1j**	**2j**	98/99
11		4-OH **1k**	**2k**	100/99
12		4-CO_2Me **1l**	**2l**	99/100
13		4-$CONH_2$ **1m**	**2m**	99/99
14		4-Ac **1n**	**2n**	98/100
15[d]		2-Ac **1o**	**2o**	98/99
16		4-NO_2 **1p**	**2p**	99/99
17		2-NO_2 **1q**	**2q**	98/99
18[d]	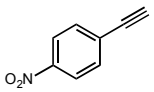	**1r**	**2r**	98/96
19[d]	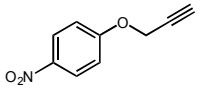	**1s**	**2s**	98/97
20	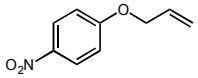	**1t**	**2t**	100/99
21	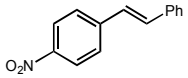	**1u**	**2u**	98/99
22[d]	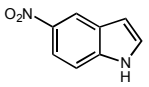	**1v**	**2v**	98/99[e]
23	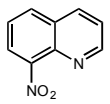	1w	**2w**	97

[a] Reaction conditions: 1 (0.4 mmol), catalyst (2 mol% Ru, 5.1%($_{81}$Ru$_{19}$Co)/PS), and NH_2NH_2•H_2O (3 equiv) in ethanol (2 ml) at ambient temp. [b] Isolated yields. [c] Run at 50 °C. [d] 4 mol% catalyst employed. [e] Run 7 h.

We found that the recovered nanoparticles could be directly reused up to five times without significant decrease in the product yields or selectivity. Importantly, no reactivation step is necessary to regenerate an active catalyst.

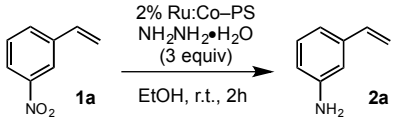

	Run 1	Run 2	Run 3	Run 4
yield/selectivity	99/97	99/96	98/97	96/96

Reactions conditions: **1a** (0.4 mmol), catalyst (2 mol% wrt Ru, 2.5:1 Ru:Co), and NH_2NH_2•H_2O (3 equiv) in EtOH at room temp.

Scheme 1. Catalyst recyclability study.

We also tested the catalysts for leaching of the metal nanoparticles into solution to determine whether the reaction was catalyzed by homogenous nanoparticles that had escaped the polymer matrix. After completion of the reduction reaction, the nanoparticle catalysts were filtered off and the metal content of the solution was determined by ICP-MS analysis. We found that only a small amount of the total ruthenium and cobalt initially added to the reaction leached out of the polymer during catalysis (1.2% and 1.3% respectively). We also removed the catalyst at partial reaction conversion (similar to the Cat-in-a-Cup test)[17] via filtration through a sintered glass funnel. After catalyst removal, we observed no further conversion to product (Figure 3). Readdition of catalyst after several hours led resumption of the reduction reaction. These results support our hypothesis that polymer-incarcerated Ru–Co nanoparticles are responsible for the observed catalysis and not homogeneous nanoparticles leached into solution from the polymer matrix.

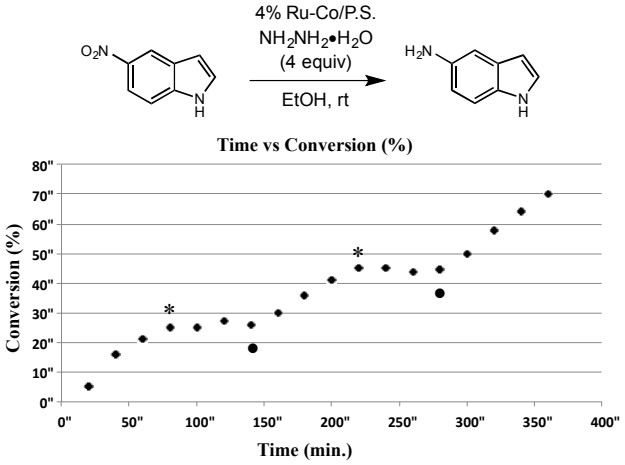

Figure 3. Test for homogeneous nanoparticles. Catalyst was removed by filtration at time points indicated with *. Catalyst was added back to the reaction at time points indicated by •.

Having demonstrated the broad scope of our nitro reduction catalyst, we desired to determine the impact of the polymer structure on catalyst activity. In the reduction of noble metals in the presence of polystyrene, it has been hypothesized that weak interactions between the metal surface and the pi electrons of the benzene rings[18] in the polymer facilitates formation of size-controlled nanoclusters and stabilizes the resulting nanoparticles towards oxidation.[19] Our hypothesis is that this weak polymer-nanoparticle interaction can be tuned by changing the electronic properties of the aromatic rings and thus have an impact on the catalytic activity of the nanoparticle catalysts.

We first synthesized polystyrene polymers containing electron-donating and electron-withdrawing substituents to vary the donor ability of the arene support (Figure 4). To our delight, we found that these variations had a dramatic influence on the catalytic activity of the bimetallic nanoparticle catalysts (Figure 3, **6a**–**6d**). Electron deficient poly(4-trifluoromethylstyrene) (**6b**) enabled rapid consumption of the starting material in just 20 minutes at room temperature (^{1}H NMR analysis). One caveat is that catalyst **6b** is soluble under the reaction conditions, which likely contributes to the in-

creased reactivity. However, with electron-rich polystyrenes, the same trend in reactivity is observed and catalysis slows down. For example, electron-rich polystyrene catalysts **6c** and **6d** required 10 h and 5.5 h respectively to proceed to completion. This result is consistent with a polymer electronic effect influencing the rate of the reduction reaction. We believe that two possible scenarios can explain this polymer-electronic effect. First, a weaker interaction between the nanoparticle surface and the arene π-electrons could lead to arene ligand dissociation from the surface, thus opening up more catalytic sites to facilitate reductions. Alternatively, the electronic properties of the polymer could directly impact the electron density at the metal surface, making the catalysts more reactive.[18]

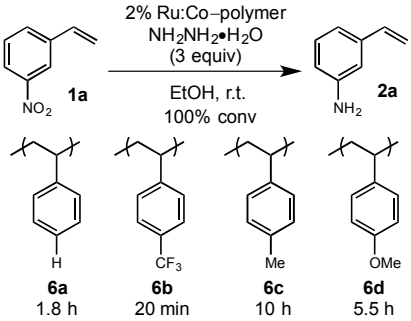

Figure 4. Electronic effects of polymer support.

In order to further explore this polymer-nanoparticle interaction, we next synthesized a variety of substituted polymers containing electron-donating functional groups (Figure 5),[12] including an amide (**6e**), a urea (**6f**), and an amine (**6g**). These functionalized polymers were designed to mimic the properties of poly(*N*-vinyl-2-pyrrolidinone) (PVP), which is widely used in nanoparticle synthesis as a polymer support. PVP is thought to influence nanoparticle stability and reactivity via coordination of the Lewis basic amide oxygen with the nanoparticle surface. These polymers followed a trend in reactivity that mimicked the trend observed with polymers **6a–6d**. While pyrrolidinone polymer **6e** provided 89% of the reduction product in 8 h, the more Lewis basic imidazolidinone polymer **6f** required 10 h to proceed to the same conversion. In addition, polymer **6g** that contains the most Lewis basic amine functionality provided only 60% of the reduction product after 10 h. This observed trend is consistent with that seen with polymers **6a–6d**, where more electron rich polymers lead to slower catalysis. These results suggest that a nanoparticle-polymer interaction is responsible for improved catalysis (vide infra) and demonstrate that the electronic properties of the polymer can be used to influence catalyst activity.

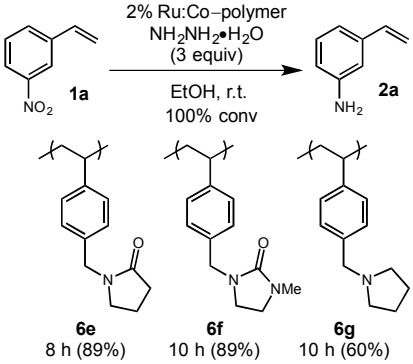

Figure 5. Impact of Lewis basic functional groups on catalysis.

Subtle changes in the reaction mechanism also support the involvement of polymer-nanoparticle interactions in modifying catalyst efficiency. When the reduction of 4-nitrostyrene **1a** is conducted with Ru:Co catalysts **6a**, **6c** or **6d–6e**, the starting material is initially converted to hydrazine **4** stoichiometrically before a significant amount of **2a** is observed (Scheme 2). Once starting material **1a** is completely consumed, hydrazine **4** is then reduced to the desired aniline **2a**. However, when electron-deficient polymer **6b** is employed, hydrazine **4** is not observed during the course of the reaction and starting material **1a** is converted directly to product **2a**. This change in the reaction dynamics could be caused by a dramatic increase in the rate of reduction of hydrazine **4** by catalyst **6b**, or by an inability of catalyst **6b** to catalyze formation of **4**. Either of these scenarios could result from a change in the electronic properties of the nanoparticles caused by variation of the supporting polymer structure.

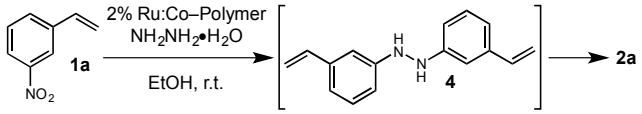

Scheme 2. Intermediate formation in nitroarene reduction.

Scanning transmission electron microscopy (STEM) images revealed that the nanoparticles in our catalysts are ~1–2 nm in diameter and exist as agglomerates in the polymer matrix that range from single particles to 30–40 nm bundles (Figure 6). The aggregation state and nanoparticle size in each of the four catalysts (**6a–6d**) are nearly identical by STEM analysis. Statistical analysis of the nanoparticle size distribution for polymeric catalysts **6a–6d** also shows nearly equal distributions in nanoparticle size for the four polymers (~1.5–2 nm diameter, see supporting information). An alternative explanation for the difference in catalytic activity between catalysts **6a–6d** could be that very subtle changes in the nanoparticle size and shape affect catalyst activity. Indeed, the trend of average particle size for catalysts **6a–6d** (CF_3 (2.0 nm) > H (1.9 nm) > OMe (1.75 nm) > Me (1.75 nm)) tracks with the observed reactivity of the nanoparticle catalysts. However, the subtle differences in nanoparticle size between catalyst **6b** (poly(4-CF_3)styrene) catalyst **6a** (polystyrene) does not explain the observed change in reaction mechanism (see Scheme 2). Thus, we believe the differences in catalyst activity for our polymer-supported nanoparticle catalysts may be due to a combination of the variations in nanoparticle size produced in each polymer support and a variation in the strength of the metal-polymer interaction.[21] The result of these polymer effects is the potential to employ modifications to polymer structure as a strategy for increasing catalyst performance, similar to what is accomplished with supporting ligands in homogeneous catalysis.

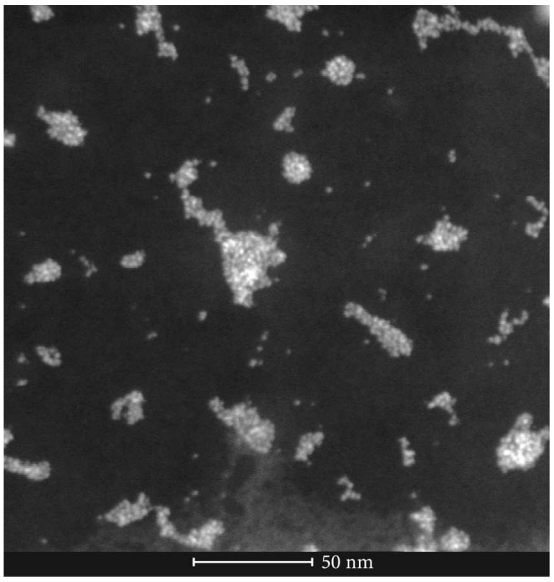

Figure 6. STEM image showing agglomerate size variation.

We have also used STEM, energy-dispersive X-ray spectroscopy (EDS), X-ray photoelectron spectroscopy (XPS), and time of flight secondary ion mass spectrometry (Tof-Sims) to investigate the composition of our nanoparticle catalysts (Figures 7a and 7b). The synthesis of Ru, Co, and Ru-Co nanoparticles by $NaBH_4$ reduction has been previously reported and our characterization data was inline with previous reports.[22] EDS linescan analysis of a single nanoparticle showed that the Ru:Co ratio remains near constant throughout the scan (Figure 7b), suggesting that ruthenium and cobalt are co-localized within the nanoparticles and not individual monometallic nanoparticles. We also used EDS to estimate the Ru:Co ratio at various locations in the nanoparticle composite, both for individual particles and large agglomerates and found the ratios to be consistent throughout the sample. We believe that the co-localization of both metals within our nanoparticle catalysts is responsible for the improved catalyst activity upon addition of cobalt to the ruthenium catalyst due to cooperativity effects. This co-localization of ruthenium and cobalt during nanoparticle formation is in accord with previous studies by Broios and coworks on the formation of ruthenium-cobalt nanoparticles.[23] XPS Analysis of our nanoparticle catalysts showed the presence of ruthenium(0) and cobalt oxide (in a +2 to +3 oxidation state) within our sample, suggesting that cobalt was not reduced during nanoparticle formation. Tof-Sims further confirmed the presence of cobalt, as well as ruthenium (a series of peaks with intensities consistent with its isotopic abundance). A rather intense tropylium ion ($C_7H_7^+$, m/z 91) was also observed, which is consistent with the organic matrix.

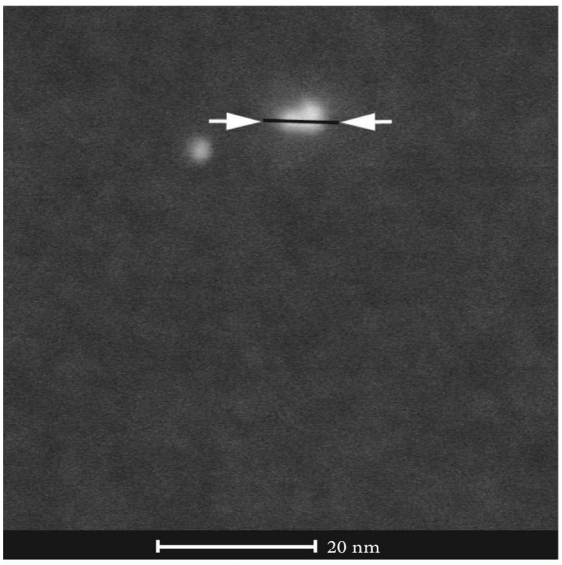

(a) STEM image showing EDS linescan location

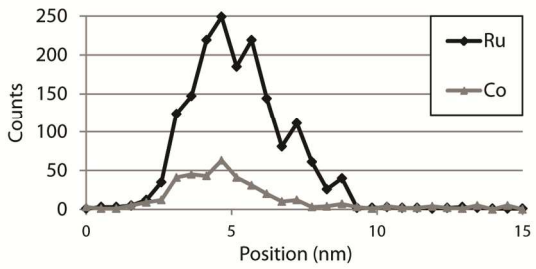

(b) EDS linescan result showing Co correlating to Ru

Figure 7. Energy-dispersive X-ray spectroscopy (EDS) Linescan of Ru-Co nanoparticles in polystyrene

Conclusion

In conclusion, we have demonstrated that both the composition (M_1:M_2 ratio) of bimetallic Ru:Co nanoparticle catalysts and the electronic structure of the supporting polymers can be varied to optimize the catalytic activity of polymer-supported nanoparticles for nitroarene reductions. This polymer-ligand approach to nanoparticle catalysis provides an attractive strategy for improving catalyst reactivity and selectivity by systematically varying the electronic structure of the polymer support. These variations in polymer structure lead to predictable changes in the catalyst activity that can be used to optimize catalyst efficiency, as is accomplished through ligand design in homogeneous catalysis. Our studies have also led to the development of readily synthesized, polymer-supported bimetallic nanoparticle catalysts that exhibit exceptional activity and chemoselectivity in nitroarene reduction reactions that occur at room temperature. These nano-composite polymer catalysts are synthesized in a single step from commercial polymers and metal salts, enable efficient and chemoselective catalysis under mild conditions, and can be recovered and reused without loss of catalytic activity.

ASSOCIATED CONTENT

Supporting Information Available: Experimental procedures, new compound characterization data, STEM Images and statistical analysis data of **6a**–**6d,** and XPS and ToF-SIMS spectra**.** This material is available free of charge via the Internet at http://pubs.acs.org.

AUTHOR INFORMATION

Corresponding Author

*e-mail: dmichaelis@chem.byu.edu

ACKNOWLEDGMENT

We thank Brigham Young University for financial support. We wish to thank Prof. Shu Kobayashi for permitting D.J.M. to perform a research exchange in his laboratories

REFERENCES

(1) For reviews, see: (a) *Nanocatalysis: Synthesis and Applications*, (eds. Polshettiwar, V.; Asefa, T.), Wiley, New Jersey, 2013. (b) Cong, H.; Porco, Jr., J. A. *ACS Catal.* **2012**, *2*, 65–70. (c) Yasukawa, T.; Miyamura, H.; Kobayashi, S. *Chem. Soc. Rev.* **2014**, *43*, 1450–1561. (d) Pachón, L. D.; Rothenberg, G. *Appl. Organometal. Chem.* ***2008,*** *22,* 288–299. (e) Astruc, D. in *Nanoparticles and Catalysis*. (Ed: D. Astruc), Wiley-VCH, Weinheim, 2008, pp. 1–48. (f) Astruc, D.; Lu, F.; Ruiz Aranzaes, J. *Angew. Chem. Int. Ed.* **2005**, *44*, 7852–7872.

(2) For reviews, see: Na, K.; Zhang, Q.; Somorjai, G. A. *J. Cluster. Sci.* **2014***, 25,* 83–114. (b) Zaera, F. *Chem. Soc. Rev.* **2013**, *42*, 2746–2762. (c) Mondloch, J. E.; Bayram, E.; Finke, R. G. *J. Mol. Catal. A: Chem.* **2012**, 355, 1–38. (d) Gates, B. C. *Chem. Rev.* **1995**, *95*, 511–522.

(3) (a) Tauster, S. J.; Fung, S. C.; Garten, R. L. *J. Am. Chem. Soc.* **1978**, *100*, 170–175.

(4) For reviews, see: (a) Serna, P.; Boronat, M.; Corma, A. *Top. Catal.* **2011**, *54*, 439–466. (b) Lim, B.; Xia, Y. *Angew. Chem. Int. Ed.* **2011**, *50*, 76–85. (c) Somorjai, G. A.; Park, J. Y. *Angew. Chem. Int. Ed.* **2008,** *47*, 9212–9228.

(5) (a) Akiyama, R.; Kobayashi, S. *Angew. Chem. Int. Ed.* **2001,** *40*, 3469–3471. (b) Akiyama, R.; Kobayashi, S. *J. Am. Chem. Soc.* **2003**, *125*, 3412–3413. For reviews, see: (c) Miyamura, H.; Kobayashi, S. *Acc. Chem. Res.* **2014**, *47*, 1054–1066. (d) Kobayashi, S.; Miyamura, H. *Aldrichimica Acta* **2013***, 46*, 3–19. (e) Kobayashi, S.; Miyamura, H. *Chem. Rec.* **2010**, *10*, 271–290. (f) Akiyama, R.; Kobayashi, S. *Chem Rev.* **2009**, *109*, 594–642. (g) Shenhar, R.; Norsten, T. B.; Rotello, V. M. *Adv. Mater.* **2005**, *17,* 657–669.

(6) (a) Soulé, J.-F.; Miyamura, H.; Kobayashi, S. *J. Am. Chem. Soc.* **2013***, 135,* 10602–10605. (b) Miyamura, H.; Morita, M.; Inasaki, T.; Kobayashi, S. *Bull. Chem. Soc. Jpn.* **2011**, *84*, 588–599. (c) Nishio, R.; Sugiura, M.; Kobayashi, S. *Org. Lett*. **2005**, *7*, 4831–4834.

(7) (a) Yuan, H.; Yoo, W.-J.; Myamura, H.; Kobayashi, S. *J. Am. Chem. Soc.* **2012***, 134*, 13970–13973. (b) Yasukawa, T.; Miyamura, H.; Kobayashi, S. *J. Am. Chem. Soc.* **2012**, *134*, 16963–16966. (c) Yuan, H.; Yoo, W.-J.; Miyamura, H.; Kobayashi, S. *Adv. Synth. Catal.* **2012**, *354,* 2899–2904. (d) Yoo, W.-J.; Miyamura, H.; Kobayashi, S. *J. Am. Chem. Soc.* **2011**, *133*, 3095–3103. (e) Miyamura, H.; Matsubara, R.; Kobayashi, S. *Chem. Commun.* **2008**, 2031–2033. (f) Kaizuka, K.; Miyamura, H.; Kobayashi, S. *J. Am. Chem. Soc.* **2010**, *132*, 15096–15098.

(8) For reviews of bimetallic nanoparticle catalysis, see: (a) Kiely, C. J.; He, Q.; Tiruvalam, R.; Dimitratos, N.; Forde M, M.; Sankar, M.; Hutchings, G. J. *Microsc. Microanal*. **2014**, *20*, 74–75. (b) Sankar, M.; Dimitratos, N.; Miedziak, P. J.; Wells, P. P. Kiely, C. J.; Hutchings, G. J. *Chem. Soc. Rev.* **2012**, *41*, 8099–8139.

(9) (a) An, K.; Somorjai, G. A. *Catal. Lett.* **2015**, *145*, 233–248. (b) Notar Francesco, I.; Fontaine-Vive, F.; Antoniotti, S. ChemCatChem **2014**, *6*, 2784–2791. (c) Calderone, V. R.; Shiju, N. R.; Curulla-Ferré, D.; Chambrey, S.; Khodakov, A.; Rose, A.; Thiessen, J.; Jess, A.; Rothenberg, G. *Angew. Chem. Int. Ed.* **2013**, *52*, 4397–4401. (d) Calderone, V. R.; Shiju, N. R.; Curulla-Ferré, D.; Rothenberg, G. *Green Chem.* **2011**, *13*, 1950–1959.

(10) (a) Vu, K. B.; Bukhryakov, K. V.; Anjum, D. H.; Rodionov, V. O. *ACS Catal.* **2015**, *5*, 2529–2533. (b) Yan, N.; Yuan, Y.; Dyson, P. J. *Dalton Trans.* **2013**, *42*, 13294–13304.

(11) Ohtaka, A.; Kuroki, R.; Teratani, T.; Shinagawa, T.; Hamasaka, G.; Uozumi, Y.; Shimomura, O.; Nomura, R. *Green and Sustainable Chem.* **2011**, *1*, 19–40.

(12) For recent examples of nanoparticle-polymer support interactions, see: (a) Zhanga, J.; Yuanc, Y.; Kilpinc, K. J.; Koua, Y.; Dyson, P. J.; Yan, N. *J. Mol. Catal. A: Chem.* **2013**, *371*, 29–35. (b) Borodko, Y.; Humphrey, S. M.;Tilley, T. D.; Frei, H.; Somorjai. G. A. *Phys. Chem. C* **2007**, *111,* 6288–6295. (c) Galow, T. H.; Drechsler, U.; Hanson, J. A.; Rotello, V. M. *Chem. Commun.* **2002**, 1076–1077.

(13) Blaser, H.-U.; Steiner, H.; Studer, M. *ChemCatChem* **2009**, *1*, 210–221. (b) Blaser, H.-U.; Siegrist, U.; Steiner, H. In *Fine Chemicals Through Heterogeneous Catalysis: Aromatic Nitro Compounds*; R. A. Sheldon, H. van Bekkum Eds.; Wiley: New York, 2001; pp. 389.

(14) For leading references, see: (a) Furukawa, S.; Yoshida, Y.; Komatsu, T. *ACS Catal*. **2014**, *4*, 1441–1451. (b) Cai, S.; Duan, H.; Rong, H.; Wang, D.; Li, L.; He, W.; Li, Y. *ACS Catal.* **2013**, *3*, 608–612. (c) Pal, J.; Mondal, C.; Sasmal, A. K.; Ganguly, M.; Negishi, Y.; Pal, T. *ACS Appl. Mater. Interfaces* **2014***, 6,* 9173–9184. (d) Zhao, Z.; Yang, H.; Li, Y.; Guo, X. *Green Chem.* **2014**, *16,* 1274–1281. (e) Jagadeesh, R. V.; Surkus, A.-E.; Junge, H.; Pohl, M.-M.; Radnik, J.; Rabeah, J.; Huan, H.; Schünemann, V.; Brückner, A.; Beller, M. *Science*, **2013**, *342,* 1073–1076. (f) Westerhaus, F. A.; Jagadeesh, R. V.; Wienhöfer, G.; Pohl, M.-M.; Radnik, J.; Surkus, A.-E.; Rabeah, J.; Junge, K.; Junge, H.; Nielsen, M.; Brückner, A.; Beller, M. *Nature Chem.* **2013**, *5*, 537–543. (g) Mitsudome, T.; Mikami, Y.; Matoba, M.; Mizugaki, T.; Jitsukawa, K.; Kaneda, K. *Angew. Chem. Int. Ed.* **2012**, *51*, 136–139.

(15) For selected examples, see: (a) Petkar, D. R.; Kadu, D. S.; Chikate, R. C. *RCS Adv.* **2014**, *4*, 8004–8010. (b) Ganji, S.; Enumula, S. S.; Marella, R. K.; Rao, K. S. R.; Burri, D. R. *Catal. Sci. Technol.* **2014**, *4*, 1813–1819. (c) He, L.; Wang, L.-C.; Sun, H.; Ni, J.; Cao, Y.; He, H.-Y.; Fan, K.-N. *Angew. Chem. Int. Ed.* **2009**, *48*, 9538–9541.

(16) (a) Carrillo, A. I.; Stamplecoskie, K. G.; Marin, M. L.; Scaiano, J. C. *Catal. Sci. Technol*. **2014**, *4*, 1989–1996. (b) Kim, J. H.; Park, J. H.; Chung, Y. K.; Park, K. H. *Adv. Synth. Catal.* **2012**, *354*, 2412–2418.

(17) Gaikwad, A. V.; Boffa, V.; ten Elshof, J. E.; Rothenberg, G. *Angew. Chem. Int. Ed.* **2008**, *47*, 5407–5410.

(18) (a) Kumar, A.; Mandal, S.; Mathew, S. P.; Selvakannan, P. R.; Mandale, A. B.; Chaudhari, R. V.; Sastry, M. *Langmuir* **2002**, *18*, 6478–6483; (b) Ramanath, G.; D□Arcy-Gall, J.; Maddaninath, T.; Ellis, A. V.; Ganesan, P. G.; Goswami, R.; Kumar, A.; Vijayamohanan, K. *Langmuir* **2004**, *20*, 5583–5587; (c) Maddanimath, T.; Kumar, A.; D□Arcy-Gall, J.; Ganesan, P. G.; Vijayamohanan, K.; Ramanath, G. *Chem. Commun.* **2005**, 1435–1437; (d) Nakazawa, M.; Somorjai, A. *Appl. Surf. Sci.* **1993**, *68*, 517–537.

(19) Miyamura, H.; Matsubara, R.; Miyazaki, Y.; Kobayashi, S. *Angew. Chem. Int. Ed.* **2007**, *46*, 4151–4154.

(20) Since very little nanoparticle leaching is observed, we do not believe that variations in polymer structure lead to higher concentrations of active soluble nanoparticle catalysts and that the polymer structure does in fact influence the catalytic properties of the catalyst.

(21) (a) An, K.; Somorjai, G. A. *Catal. Lett.* **2015**, *145*, 233–248. (b) Notar Francesco, I.; Fontaine-Vive, F.; Antoniotti, S. ChemCatChem **2014**, *6*, 2784–2791. (c) An, K.; Somorjai, G. A. *ChemCatChem* **2012**, 4, 1512–1524. (d) Vu, K. B.; Bukhryakov, K. V.; Anjum, D. H.; Rodionov, V. O. *ACS Catal.* **2015**, *5*, 2529–2533.

(22) (a) Glavee, G. N.; Klabunde, K. J.; Sorensen, C. M.; Hadjipanayis, G. C. *Inorg. Chem.* **1993**, *32*, 474–477. (b) Soulé, J.-F.; Miyamura, H.; Kobayashi, S. *J. Am. Chem. Soc.* **2011**, *133*, 18550–18553. (c) Liang, X.; Zhao, L. *RSC Advances* **2012**, *2*, 5485–5487. (d) Chowdhury, A. D.; Agnihotri, N.; De, A. *Chem. Eng. J.* **2015**, *264*, 531–537.

(23) Hong, J.; Marceau, E.; Khodakov, A. Y.; Gaberová, L.; Griboval-Constant, A.; Girardon, J.-S.; La Fontaine, C.; Briois, V. *ACS Catal.* **2015**, *5,* 1273–1282.

Insert Table of Contents artwork here